Appl. Phys. B 81, 753–756 (2005)
DOI: 10.1007/s00340-005-1966-3

Applied Physics B
Lasers and Optics

Rapid communication

F. TAVELLA[1]
K. SCHMID[1,2]
N. ISHII[1]
A. MARCINKEVIČIUS[1,✉]
L. VEISZ[1]
F. KRAUSZ[1,2]

High-dynamic range pulse-contrast measurements of a broadband optical parametric chirped-pulse amplifier

[1] Max-Planck Institut für Quantenoptik, Hans-Kopfermann-Straße 1, 85748 Garching, Germany
[2] Department für Physik, Ludwig-Maximilians-Universität München, Am Coulombwall 1, 85748 Garching, Germany

Received: 20 July 2005
Published online: 14 September 2005 •

ABSTRACT We report on the pulse contrast-ratio characterization of a few-cycle 0.2 TW optical parametric chirped pulse amplifier system operating at 20 Hz. A specially designed third-order correlator was used to characterize and optimize the contrast of the system. We demonstrate that the pulse contrast depends much more on the temporal overlap between the pump and the seed pulse than the shape of the amplified spectrum. The best amplified pulse contrast-ratio was 10^{-4} at $\Delta t = \pm 25$ ps and $> 10^{-9}$ at $\Delta t = \pm 150$ ps delays.

PACS 42.65.Vj; 42.65.Re

1 Introduction

The temporal intensity profile of high intensity laser pulses over a large dynamic range is a major concern in various solid-target experiments especially for high-order harmonics generation [1], isochoric heating [2], and ion-acceleration from thin film experiments [3]. Pre-pulses and pedestal can significantly alter the interaction because they can reach considerable intensities in such lasers, whereas the post-pulses are amplified reflections of the main pulse and are of less importance for many high-intensity experiments. In chirped-pulse laser amplifiers the amplified spontaneous emission generates a long pedestal, spectral clipping and phase distortions lead to an additional background near the main pulse [4]. In optical parametric chirped pulse amplifiers (OPCPA), the pump pulse duration is of similar length as the signal pulse in the amplifier. Since there is no gain outside this time window, only the pedestal caused by parametric superfluorescence which is within the gain time window will be amplified [5]. Optical parametric superfluorescence results from the spontaneous decay of a pump photon into an idler and a signal photon and due to subsequent amplification this process becomes significant at high pump intensities. Although the intensity of the superfluorescence is usually orders of magnitude smaller than that of the main peak, it cannot be ignored in many experiments. Similarly to the conventional chirped pulse amplifiers, OPCPA also suffers from the formation of amplified post-pulses. They originate from the doubly internally reflected (DIR) seed pulses inside the nonlinear crystal. The temporal separation of the main pulse and the post-pulse (t_{DIR}) is determined by the ratio of twice the crystal length and the group velocity of the signal. It is clear that the efficient amplification of the DIR pulse is possible if the pump pulse duration is longer than t_{DIR}. The first attempt to characterize the amplified pulse contrast ratio of the narrowband OPCPA was made by Yoshida et al. [6] where the pre-pulse ratio of $> 10^{-8}$ at $\Delta t \sim 500$ ps delays was measured using a photodiode. In the recent work of Jovanovic et al. [7] the pre-pulse contrast level of $> 10^{-7}$ of the 200 fs pulses was measured.

Despite a high activity in the field of high-power broadband OPCPA systems development [8–10], the pulse-contrast characterization of high energy, few-cycle pulses was until now not clearly demonstrated. The goal of this paper is to investigate the pulse contrast of the multi-millijoule, sub-10 fs pulses from a broadband OPCPA, to clarify the existence of amplified DIR pulses, and to study the influence of the delay between the seed and the pump on the amplified pulse contrast. We present to our knowledge the first high-dynamic range pulse-contrast measurements of such a system and demonstrate thereby its high potential for future high-intensity ultrashort pulse amplifiers.

2 Experimental setup

2.1 *OPCPA*

The experiments were performed with an OPCPA-system similar to that described by Ishii et al. [9]. For OPCPA pumping we used a picosecond Nd:YAG amplifier which produces 30 mJ frequency doubled 532-nm pulses, at a repetition rate of 20 Hz. This amplifier was seeded by an actively mode-locked 90-ps Nd:YVO_4 oscillator with its repetition rate synchronized to an external rf clock. The broadband seed pulses from the Ti:Sapphire oscillator are temporally stretched to a duration of 50 ps with a negative-dispersion stretcher and subsequently amplified in two double-pass OPCPA stages. The oscillator spectrum after the stretcher and the amplified pulse spectrum are depicted in Fig. 1(a) and (b), respectively. In the first stage we used a 4.4-mm thick,

✉ Fax: +49-89-32905-200, E-mail: andrius.marcinkevicius@mpq.mpg.de

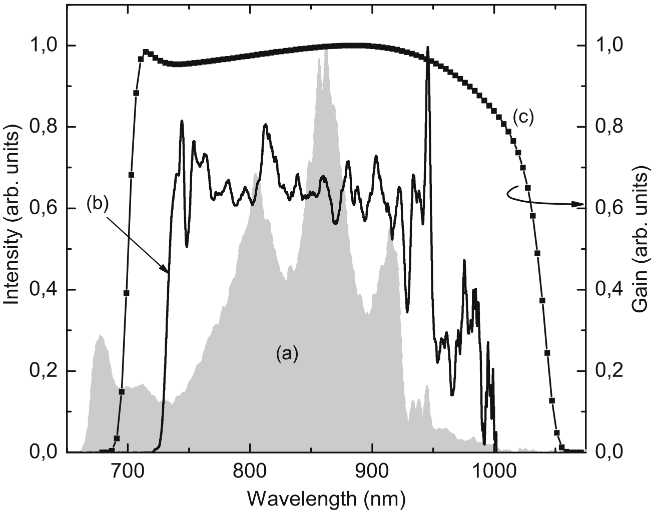

FIGURE 1 Measured spectra of the seed pulses after the stretcher (**a**), amplified signal at the OPCPA output (**b**). The *curve* (**c**) depicts the calculated gain of 4 mm BBO

type-I, antireflection-coated, BBO crystal with the internal non-collinearity angle between the pump and the seed of 2.3°.

During the alignment of the amplifier we tried to reduce the amount of superfluorescence by decreasing the pump intensity and monitoring the output energy after the first stage when the seed was blocked. At an incident pump intensity of approximately 24 GW/cm^2 and with the seed light blocked the measured superfluorescence energy after the first stage was smaller than 100 nJ. Seeding this amplifier stage with a 200 pJ pulse resulted in an output energy of 100-μJ, corresponding to a gain of 5×10^5.

In the second stage we used a 5.5-mm thick BBO crystal. With the pump pulse of an intensity of approximately 10 GW/cm^2 passed twice through the crystal, the amplified pulse energy reached 3 mJ, whereas single-pass pumping resulted in 1.5 mJ. Thus in the two OPCPA stages we obtained a total gain of the order of 10^7. With the maximal available pump intensity we were able to reach a peak pump-to-signal conversion efficiency of 18% without a deep saturation of the parametric gain. In spite of this fact, we achieved an energy stability of the amplified pulses better than 6% RMS, owing to a pump energy stability of 1.5% RMS. The amplified pulses were compressed using a combination of a bulk-material compressor consisting of SF57 and fused silica blocks and a set of four positive-dispersion dielectric mirrors. Feeding back the residual spectral phase measured by a SPIDER interferometer to an acousto-optic pulse shaper DAZZLER [11], we achieved recompression of the amplified pulses to slightly less than 10 fs (FWHM). The numerically calculated parametric amplification bandwidth (Fig. 1(c)) indicates that broadband spectrum leading to 6.1 fs pulses can be amplified.

2.2 *Third-order correlator*

There exist different methods of characterizing the contrast of ultra-short-laser pulses with high-dynamic range which also allow one to distinguish between pre- and post-pulses. In the case of OPCPA systems, one can use the OPCPA crystal itself to perform the measurement [12], use third-harmonic generation (THG) on interfaces between transparent optical media [13] or non-collinear THG subsequently using two nonlinear crystals [14, 15].

For pulse contrast measurements we developed a third-order correlator with a scanning range of > 600 ps and a dynamic range of > 10^9. The optical layout of the third-order correlator is sketched in Fig. 2. The correlator is based on type-I phase-matched second harmonic generation, followed by the third harmonic generation (SHG and THG, respectively) in BBO crystals. The bandwidth of the optical components in the correlator did not allow us to make reliable statements about the time structure within less than 90 fs. We used only reflective optics and uncoated, wedged 100-μm-thick BBO-crystals to minimize pulse broadening and increase phase-matching bandwidth. Even 10-μm-thick BBO crystals can be used to measure the pulse duration directly at the expense of decreased measurable dynamic-range. To avoid saturation of the detector near the pulse peak, we implemented a variable attenuator, based on the mirrors M1 and M2, which are only partially coated with silver and are mounted on motorized translation stage T1 (Fig. 2). In this way, the incident beam is either reflected by two silver mirrors, by one silver mirror and one glass surface or by two glass surfaces, depending on the position of translation stage T1. This implies that

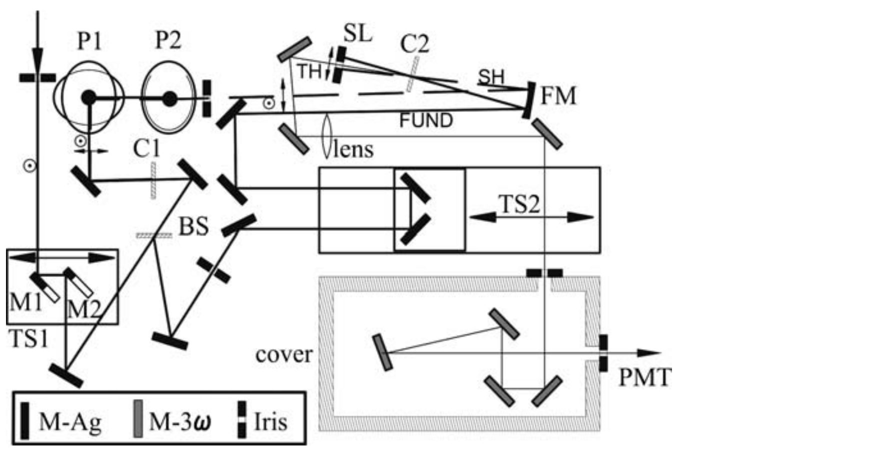

FIGURE 2 Optical layout of the third-order correlator. TS1: translation stage; M1, M2: Mirrors which are only partially coated; BS: pellicle beam splitter; C1: SHG crystal; M-Ag: Ag-broadband mirrors; P1: Periscope; P2: height-change. P1 and P2 equipped with dichroic mirrors for SH; FM: focussing mirror, $f = 100$ mm; M-3ω: dielectric mirrors for TH; C2: THG crystal; SL: slit; lens: $f = 100$ mm; TS2: translation stage for time delay; PMT: solar-blind photomultiplier tube

for s-polarized light at a incident angle of 45° the energy of the pulses can be reduced to approximately 10% and 1% by one or two reflections off the glass plate, respectively. The TH signal was then recorded by a Hamamatsu R2078-2 solar-blind photomultiplier tube (PMT) with very low dark current. Variation of the voltage applied to the PMT and the incoming pulse-energy (by means of translation stage TS1) together with careful suppression of the background through the whole correlator allowed to reach a dynamic range of nine orders of magnitude at a pulse energy as low as 700 μJ.

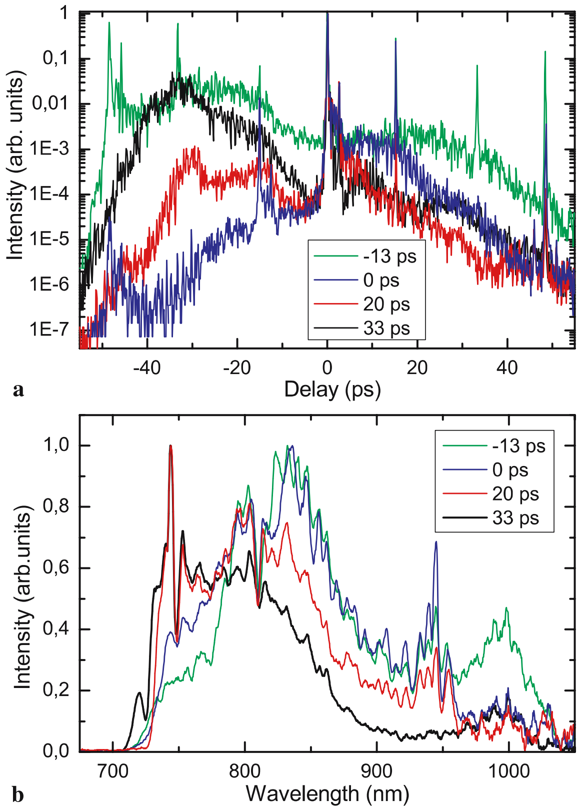

FIGURE 3 Dependencies of the pulse contrast (**a**) and amplified pulse spectra (**b**) on the delay between pump and seed. Zero delay corresponds to the delay when the highest pulse contrast was observed, the positive delay means that pump pulse precedes the seed pulse

3 Results and discussion

One of the main conclusions from our measurements has been that the delay between the seed- and the pump-pulse strongly influences the pulse contrast-ratio. To investigate the contrast near the main pulse in more detail, we limited the scanning range of the correlator to ±55 ps. For this measurement only one pass was used in the second OPCPA stage, yielding an amplified pulse energy of 1.5 mJ, less than 10% (130 μJ) of which was used for the correlation measurements. The results are summarized in Fig. 3a, which depicts four autocorrelation traces recorded at different delays between seed and pump pulse. The zero delay between the pump and the seed pulse corresponds to a delay setting where the contrast between the main pulse and superfluorescence background was highest. For this delay setting on the leading edge of the pulse, contrast is equal to $\sim 10^{-4}$. In a third-order correlation, every pre-pulse (post-pulse) will generate a peak at positive (negative) delays as well, but this "ghost" will be of smaller amplitude than the peak at the real position of the satellite. In a correlation-trace which is normalized to one, the contrast ratio between the main pulse and the ghost pulse is given approximately by the square of the true contrast of the satellite. We attribute the post-pulse appearing at +48.5 ps to the DIR pulse in the 4.4 mm BBO crystal of the first stage which was further amplified in the second pass in the first stage as well as in the second stage. The post-pulse appearing at +15.3 ps was identified as resulting from parasitic reflection inside the pulse stretcher. Interestingly, that at a seed delay of −13 ps the DIR pulse was more amplified than the main pulse and this post-pulse causes the very high peak at 48.5 ps in the correlation trace. Moreover, the additional peaks at ±33.2 ps were identified as measurement artifacts coming from the correlation of the strong post-pulse at 48.5 ps with the post-pulse at 15.3 ps. This measurement allows us to conclude that delaying of the seed pulse with respect to the pump pulse facilitates more efficient amplification of parametric fluorescence in the pulse front and causing deterioration of the main pulse contrast (Fig. 3a). Furthermore, with the increasing seed delay the pedestal energy redistribution from the trailing-edge to the leading-edge of the pulse is clearly evident.

Together with the correlation measurements we measured amplified pulse spectra for different seed delays (Fig. 3b). It can be seen that for a delay of 33 ps the spectrum of the amplified pulses becomes narrower, and is shifted towards shorter wavelengths, whereas for −13 ps we observed stronger amplification in the near-infrared. This indicates that the amplified pulse spectrum is also sensitive to the pump-seed temporal overlap, particularly for the long seed delays, and that the sharp edge near the 700 nm or spectral components appearing around 1 μm in the amplified spectrum indicates presence of the stronger superfluorescence background. However, due to the high sensitivity of the amplified spectrum on the system alignment it is impossible to assess the amplified pulse contrast-ratio from the spectral measurements.

We have also performed measurements over an increased scanning range by using the maximum output of the system. These measurements, reveal a second post-pulse at +61.5 ps, which stems from the 5.5 mm BBO crystal in the second stage (Fig. 4). The same post-pulses cause another series of two DIR pulses in the second pass of the second stage which appears in the correlation trace at 110 ps and 123 ps. The broad pedestal from −55 ps to +55 ps in the third order correlations depicted in Figs. 3 and 4 originates from parametric fluorescence generated and amplified in the OPCPA stages. The background between 65 ps and 150 ps with approximately 10^{-6} pulse contrast is attributed to the double reflection in the second BBO crystal of the pedestal produced in the first stage. The measurement was performed with 700 μJ of the

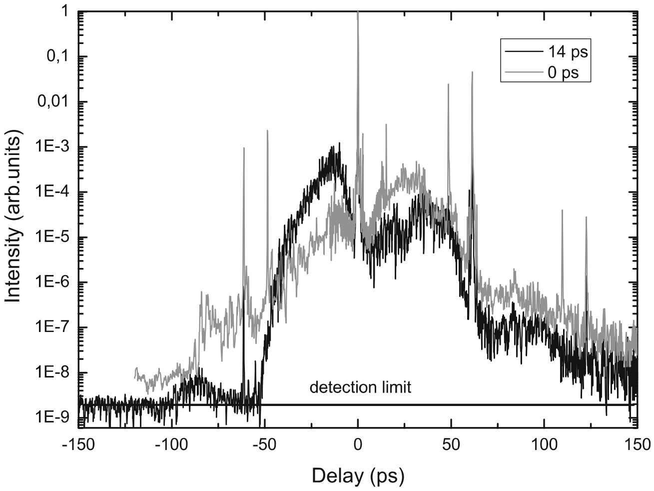

FIGURE 4 Long scanning range third-order correlations recorded at two different pump-seed delays

3 mJ pulses coupled into the correlator. At this energy, the dynamic range of the correlator is 9 orders of magnitude, allowing the conclusion that OPCPA contrast at large delays is equal to or better than that. It can also be seen that the best pulse-contrast obtained in these measurements is larger than four orders of magnitude at ±25 ps.

By integrating the respective parts of the correlations, it is possible to estimate the energy content of the pedestal and of the main pulse. The energy content of the main pulse for the 0 ps pump-seed delay in Fig. 4 is > 75%, with the leading part of the pedestal from −100 ps to −0.1 ps carrying less than 1.4%. In the non-optimized case, 5% of the energy is in the leading part of the pedestal and the main pulse contains 93%. At this delay between seed and pump pulses the amplification of the DIR pulses is thus much less pronounced. So at least in our current OPCPA system, there seems to exist a trade off between the energy in the main pulse and the contrast between main pulse and pedestal, because for high contrast it is necessary to shift the seed more to the leading part of the pump pulse, which will result then in stronger post-pulses. One possibility to suppress amplification of the DIR pulses is development of the lower reflectivity broadband antireflection coatings for the BBO crystals. Further investigations on OPCPA pulse contrast improvement is underway.

In conclusion, we have measured the pulse contrast ratio of a broadband OPCPA system using a high-dynamic range third-order correlator. The temporal structure of the OPCPA output in the ps time scale consists of a broad pedestal and several post-pulses. We have shown that some of these post-pulses are amplified and thus inherent to all OPCPA systems. Maximal measured pulse contrast ratios of 10^{-4} and $> 10^{-9}$ in the temporal windows of ±25 ps and ±150 ps, respectively, were obtained. The contrast of the pulse front has been found to be sensitively dependent on the delay between the seed and the pump pulse.

ACKNOWLEDGEMENTS This work is partially supported by Euroatom-IPP grant, LASERLAB-Europe and DFG-Project SFB Transregio TR 18.

REFERENCES

1 M. Zepf, G.D. Tsakiris, G. Pretzler, I. Watts, D.M. Chambers, P.A. Norreys, U. Andiel, A.E. Dangor, K. Eidmann, C. Gahn, A. Machacek, J.S. Wark, K. Witte: Phys. Rev. E **58**, R5253 (1998)
2 A. Saemann, K. Eidmann, I.E. Golovkin, R. Mancini, E. Andersson, E. Forster, K. Witte: Phys. Rev. Lett. **82**, 4843 (1999)
3 M. Kaluza, J. Schreiber, M. Santala, G. Tsakiris, K. Eidmann, J.M. ter Vehn, K. Witte: Phys. Rev. Lett. **93**, 045 003 (2004)
4 J. Itatani, J. Faure, M. Nantel, G. Mourou, S. Watanabe: Opt. Commun. **148**, 70 (1998)
5 I.N. Ross, P. Matousek, M. Towrie, A.J. Langley, J.L. Collier: Opt. Commun. **144**, 125 (1997)
6 H. Yoshida, E. Ishii, R. Kodama, H. Fujita, Y. Kitagawa, Y. Izawa, T. Yamanaka: Opt. Lett. **28**, 257 (2003)
7 I. Jovanovic, C.G. Brown, Ch.A. Ebbers, C.P.J. Barty, N. Forget, C. Le Blanc: Opt. Lett. **30**, 1036 (2005)
8 P. Schlup, J. Biegert, C.P. Hauri, G. Arisholm, U. Keller: Appl. Phys. B **79**, 285 (2004)
9 N. Ishii, L. Turi, V.S. Yakovlev, T. Fuji, F. Krausz, A. Baltuska, R. Butkus, G. Veitas, V. Smilgevicius, R. Danielius, A. Piskarskas: Opt. Lett. **30**, 567 (2005)
10 R.Th. Zinkstok, S. Witte, W. Hogervorst, K.S.E. Eikema: Opt. Lett. **30**, 78 (2005)
11 F. Verluise, V. Laude, Z. Cheng, Ch. Spielmann, P. Tournois: Opt. Lett. **25**, 575 (2000)
12 E.J. Divall, I.N. Ross: Opt. Lett. **29**, 19, 2273 (2004)
13 D. Meshulach, Y. Barad, Y. Silberberg: J. Opt. Soc. Am. B **14**, 2122 (1997)
14 S. Luan, M.H.R. Hutchinson, R.A. Smith, F. Zhou: Meas. Sci. Technol. **4**, 1426 (1993)
15 A. Antonetti, F. Blasco, J.P. Chambaret, G. Cheriaux, G. Darpentigny, C. Le Blanc, P. Rousseau, S. Ranc, G. Rey, F. Salin: Appl. Phys. B **65**, 197 (1997)